



HAL
open science

Expression, purification and crystallization of two endonuclease III enzymes from *Deinococcus radiodurans*.

Aili Sarre, Mats Okvist, Tobias Klar, Elin Moe, Joanna Timmins

► **To cite this version:**

Aili Sarre, Mats Okvist, Tobias Klar, Elin Moe, Joanna Timmins. Expression, purification and crystallization of two endonuclease III enzymes from *Deinococcus radiodurans*.. Acta Crystallographica Section F: Structural Biology and Crystallization Communications, 2014, 70 (Pt 12), pp.1688-92. hal-01093359

HAL Id: hal-01093359

<https://hal.univ-grenoble-alpes.fr/hal-01093359>

Submitted on 10 Dec 2014

HAL is a multi-disciplinary open access archive for the deposit and dissemination of scientific research documents, whether they are published or not. The documents may come from teaching and research institutions in France or abroad, or from public or private research centers.

L'archive ouverte pluridisciplinaire **HAL**, est destinée au dépôt et à la diffusion de documents scientifiques de niveau recherche, publiés ou non, émanant des établissements d'enseignement et de recherche français ou étrangers, des laboratoires publics ou privés.

Acta Crystallographica Section F

**Structural Biology
Communications**

ISSN 2053-230X

Expression, purification and crystallization of two endonuclease III enzymes from *Deinococcus radiodurans*

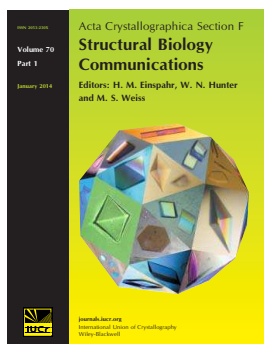
Aili Sarre, Mats Ökvist, Tobias Klar, Elin Moe and Joanna Timmins

Acta Cryst. (2014). **F70**, 1688–1692

Copyright © International Union of Crystallography

Author(s) of this paper may load this reprint on their own web site or institutional repository provided that this cover page is retained. Republication of this article or its storage in electronic databases other than as specified above is not permitted without prior permission in writing from the IUCr.

For further information see <http://journals.iucr.org/services/authorrights.html>



Acta Crystallographica Section F: Structural Biology Communications is a rapid all-electronic journal, which provides a home for short communications on the crystallization and structure of biological macromolecules. Structures determined through structural genomics initiatives or from iterative studies such as those used in the pharmaceutical industry are particularly welcomed. Articles are available online when ready, making publication as fast as possible, and include unlimited free colour illustrations, movies and other enhancements. The editorial process is completely electronic with respect to deposition, submission, refereeing and publication.

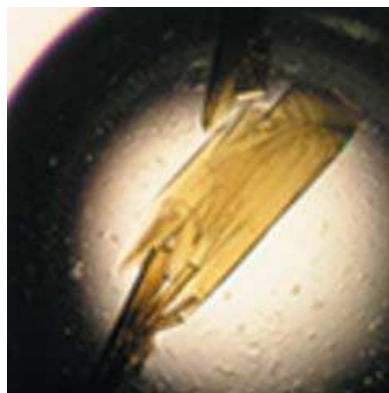
Crystallography Journals **Online** is available from journals.iucr.org

Aili Sarre,^a Mats Ökvist,^b
Tobias Klar,^b Elin Moe^{a,c,*} and
Joanna Timmins^{b,d,e,f,*}

^aChemistry Department, NorStruct, UiT The Arctic University of Norway, Forskningsparken 3, 9037 Tromsø, Norway, ^bStructural Biology Group, European Synchrotron Radiation Facility, 71 Avenue des Martyrs, 38043 Grenoble, France, ^cInstituto de Tecnologia Química e Biológica, Universidade Nova de Lisboa, Avenida da República (EAN), 2780-157 Oeiras, Portugal, ^dInstitut de Biologie Structurale, Université Grenoble Alpes, 38044 Grenoble, France, ^eInstitut de Biologie Structurale, CNRS, 38044 Grenoble, France, and ^fInstitut de Biologie Structurale, CEA, 38044 Grenoble, France

Correspondence e-mail: elin.moe@uit.no,
joanna.timmins@ibs.fr

Received 4 September 2014
Accepted 13 November 2014



© 2014 International Union of Crystallography
All rights reserved

Expression, purification and crystallization of two endonuclease III enzymes from *Deinococcus radiodurans*

Endonuclease III is a bifunctional DNA glycosylase that removes a wide range of oxidized bases in DNA. *Deinococcus radiodurans* is an extreme radiation-resistant and desiccation-resistant bacterium and possesses three genes encoding endonuclease III enzymes in its genome: DR2438 (EndoIII-1), DR0289 (EndoIII-2) and DR0982 (EndoIII-3). Here, EndoIII-1 and an N-terminally truncated form of EndoIII-3 (EndoIII-3 Δ 76) have been expressed, purified and crystallized, and preliminary X-ray crystallographic analyses have been performed to 2.15 and 1.31 Å resolution, respectively. The EndoIII-1 crystals belonged to the monoclinic space group *C*2, with unit-cell parameters $a = 181.38$, $b = 38.56$, $c = 37.09$ Å, $\beta = 89.34^\circ$ and one molecule per asymmetric unit. The EndoIII-3 Δ 76 crystals also belonged to the monoclinic space group *C*2, but with unit-cell parameters $a = 91.47$, $b = 40.53$, $c = 72.47$ Å, $\beta = 102.53^\circ$ and one molecule per asymmetric unit. The EndoIII-1 structure was determined by molecular replacement, while the truncated EndoIII-3 Δ 76 structure was determined by single-wavelength anomalous dispersion phasing. Refinement of the structures is in progress.

1. Introduction

Deinococcus radiodurans is an extremophilic bacterium that is able to withstand high doses of ionizing radiation, which introduce many diverse lesions into the DNA, including lethal double-strand breaks but also numerous base modifications such as alkylation, oxidation and deamination (Sutherland *et al.*, 2000; Ward, 1988). Many factors could contribute to the innate resistance of *D. radiodurans* to DNA damage, such as a high genome copy number (between four and ten copies during the exponential phase of growth) and an efficient DNA-repair pathway (Battista, 1997).

Repair of base modifications is carried out by the base excision repair (BER) pathway (Krokan & Bjørås, 2013). The pathway is initiated by DNA glycosylases, which recognize the damaged bases and remove them by hydrolyzing the N-glycosidic bond between the base and the sugar phosphate backbone, thereby generating an abasic site. The next step is performed by apurinic (AP) endonucleases, DNA polymerases and DNA ligases. Some of the DNA glycosylases are bifunctional and contain an AP lyase activity in addition to their N-glycosidic activity and are not dependent upon the lyase activity of AP endonucleases or DNA polymerases in order to complete the repair.

This is the case for endonuclease III (EndoIII) enzymes, a family of bifunctional DNA glycosylases that recognize and remove oxidized pyrimidines, such as thymine glycol, from damaged DNA. These enzymes are highly conserved throughout the three kingdoms of life. Unlike most other organisms, the genome of *D. radiodurans* encodes an expanded number of DNA glycosylases, including three endonuclease III enzymes (named EndoIII-1, EndoIII-2 and EndoIII-3). EndoIII-1 corresponds to the protein encoded by gene DR2438, EndoIII-2 to that encoded by DR0289 and EndoIII-3 to that encoded by DR0928 (Makarova *et al.*, 2001). Our sequence alignment analyses reveal that EndoIII-1 shares 30 and 32% sequence identity with EndoIII-2 and EndoIII-3, respectively, and EndoIII-2 and EndoIII-3 share 34% sequence identity. *D. radiodurans* EndoIII-2 displays the highest similarity to *Escherichia coli* EndoIII, sharing 43% sequence identity.

Table 1
Macromolecule-production information.

Protein	EndoIII-1	EndoIII-3Δ76
Source organism	<i>D. radiodurans</i> R1	<i>D. radiodurans</i> R1
DNA source	Genomic DNA	Genomic DNA
Expression vector	pDest14 (N-terminal His tag encoded by the forward PCR primer)	pDest14 (N-terminal His tag and TEV cleavage site encoded by the forward PCR primer)
Expression host	<i>E. coli</i> strain BL21 (DE3) pLysS	<i>E. coli</i> strain BL21 (DE3) pLysS
Complete amino-acid sequence of the construct produced	MHHHHHTLFGDVSQKGAAPLNAARPAEERAAALLAWVKERLHEEYGDQDPTPRRDPM-HELISTILSQRTTHADEEAAAYQELRDLGWDAITLAPTDVAHAIRRSNYPESK-APRIQETLRRKAAPGGYDLDFLRDLVVKDALKWLDLPGVGKVTASLVLLFNYP-ARPVFPVDTHVHRVSTRVGVIPRMGEQAHRALLALLPPDPPLYELHINFLSH-GRQVCTWTRPKCGKCILRERCDAYALYDGVKPSFSEKPKVKGKPAKG	MHHHHHENLYFQGAVPSRSPQASSKSRPLSEQNPPPVWFGEYLSRLRDTYAPELP-PPRQFPDPLGGLIRTILSQNTRRVAQRQWEVLATYPQWEAALLDGPDPGIEAT-LKSAGGGLSRMKADYIYGILAHLQEHGGLSLRFLEFPHTPEGHEQARQALAA-LPGVGHKTVALVLLFDLRRPAMPVDGNMERAARKRELVPAAWNSHKVERWYAEV-MPADWETRPFALHISGVRHGRDTRCSKHPLCPQCPLREFCPSASIFELGEAGERE-PSELEW

Table 2
Crystallization conditions.

Protein	EndoIII-1	EndoIII-3Δ76
Method	Hanging-drop vapour diffusion	Hanging-drop vapour diffusion
Plate type	24-well plate	24-well plate
Temperature (K)	293	293
Protein concentration (mg ml ⁻¹)	5.8 and 11.8	6 and 12
Buffer composition of protein solution	0.05 M Tris-HCl pH 7.5, 0.15 M NaCl, 0.2 M imidazole	0.05 M Tris-HCl pH 8.5, 0.15 M NaCl
Composition of reservoir solution	1.0 M succinic acid pH 7.0, 0.1 M HEPES pH 7.0, 1% (w/v) PEG MME 2000	0.1 M MES pH 6.5, 1.4 M ammonium sulfate, 0.01 M cobalt(II) chloride hexahydrate
Volume and ratio of drop	1 µl protein solution + 1 µl reservoir solution	2 µl protein solution + 2 µl reservoir solution
Volume of reservoir (µl)	500	500

N-terminally truncated EndoIII-3 (EndoIII-3Δ76) and full-length EndoIII-1 were cloned, expressed, purified and crystallized. Structure determination of these enzymes will contribute to a better understanding of the unusual DNA repair repertoire and outstanding radiation-resistance phenotype of *D. radiodurans*.

2. Materials and methods

2.1. Sequence amplification and cloning

The gene encoding EndoIII-1 (residues 1–259) was amplified by PCR and cloned into pDest14 (Invitrogen), and a noncleavable N-terminal hexahistidine tag (encoded by the PCR primers) was inserted upstream of the gene (Table 1). A construct corresponding to an N-terminally truncated form of EndoIII-3 (EndoIII-3Δ76) lacking the nonconserved N-terminal region (residues 1–75) was cloned into pDest14 (Invitrogen) and both an N-terminal hexahistidine tag and a TEV protease cleavage site (encoded by the PCR primers) were inserted upstream of the gene, as described previously (Moe *et al.*, 2012; Table 1).

2.2. Protein expression

Plasmids encoding EndoIII-1 and EndoIII-3Δ76 were transformed into *E. coli* strain BL21 (DE3) pLysS (Table 1). Cells were grown in LB (lysogeny broth) medium with 100 µg ml⁻¹ ampicillin and 34 µg ml⁻¹ chloramphenicol. Overnight precultures were grown at 310 K and used to inoculate a 1 l culture. Cultures were grown at 310 K until the OD₆₀₀ reached 0.7–0.9. Expression was induced with 0.5 mM isopropyl β-D-1-thiogalactopyranoside (IPTG) at 293 K overnight. Cells were harvested by centrifugation at 7548g for 25 min and resuspended in 20 ml buffer 1 (150 mM NaCl, 50 mM Tris-HCl pH 7.5) for EndoIII-1 or 20 ml buffer 2 (150 mM NaCl, 50 mM Tris-HCl pH 8.5) for EndoIII-3Δ76, and were then flash-frozen and stored at 253 K. Cells were lysed by multiple freeze–thaw cycles (alternating 298 K water bath and liquid nitrogen) in the presence of lysozyme and DNaseI. Protease-inhibitor tablets (Roche) were included in the lysis buffers. The lysates were cleared by centrifugation at 48 385g for

25 min at 277 K and the supernatants were carefully removed and used for subsequent chromatography steps.

2.3. EndoIII-1 purification and crystallization

Supernatant containing EndoIII-1 was loaded onto 1 ml Superflow Ni-NTA (Qiagen) resin pre-equilibrated in buffer 1. The resin was then washed with buffer 1, buffer 1 containing 1 M NaCl and buffer 1 supplemented with 25 mM imidazole before eluting EndoIII-1 with a linear 25–500 mM imidazole gradient. The purity of the fractions was analysed by SDS-PAGE and the peak fractions were pooled and concentrated to 11.8 mg ml⁻¹.

Initial crystallization screening was performed at 293 K by sitting-drop vapour diffusion in Greiner CrystalQuick plates. A Cartesian PixSys 4200 crystallization robot (High Throughput Crystallization Laboratory at EMBL Grenoble) was used in order to test 576 different crystallization conditions (using the method described in Dimasi *et al.*, 2007). The following commercial screens (Hampton Research) were set up: Crystal Screen, Crystal Screen 2, Crystal Screen Lite, PEG/Ion, MembFac, Natrix, Quick Screen, Grid Screens (Ammonium Sulfate, Sodium Malonate, Sodium Formate, PEG 6K, PEG/LiCl, MPD) and Index. Crystals were obtained in several conditions and the most promising ones, from the Index screen, were used as a starting point for manual optimization using the hanging-drop method at 293 K. Crystals of EndoIII-1 were grown in droplets consisting of 1 µl protein solution (at both 5.8 and 11.8 mg ml⁻¹) and 1 µl reservoir solution after 1–2 d of equilibration against 500 µl reservoir in the well. Crystals giving the best diffraction data were obtained directly from Index screen condition No. 34 [1.0 M succinic acid pH 7.0, 0.1 M HEPES pH 7.0, 1% (w/v) PEG MME 2000] at 293 K (Table 2).

2.4. EndoIII-3Δ76 purification and crystallization

Supernatant containing EndoIII-3Δ76 was loaded onto 1 ml Superflow Ni-NTA (Qiagen) resin pre-equilibrated in buffer 2. The resin was then washed with buffer 2, buffer 2 containing 1 M NaCl and buffer 2 supplemented with 40 mM imidazole before eluting

Table 3
Data-collection parameters.

	EndoIII-1 (peak)	EndoIII-3Δ76 (peak)	EndoIII-3Δ76 (remote)	
			Data set 1 (low resolution)	Data set 2 (high resolution)
X-ray source	ESRF beamline ID23-1	ESRF beamline ID23-1	ESRF beamline ID23-1	
Wavelength (Å)	1.735	1.735	1.078	
Temperature (K)	100	100	100	
Detector	ADSC Q315	ADSC Q315	ADSC Q315	
Crystal-to-detector distance (mm)	105.1	111.1	244.0	144.0
Rotation range per image (°)	0.70	0.50	2.25	1.40
Total rotation range (°)	560	720	472.5	336
Exposure time per image (s)	0.7	0.1	0.1	0.1

Table 4
Data statistics.

Values in parentheses are for the outer shell.

	EndoIII-1 (peak)	EndoIII-3Δ76 (peak)	EndoIII-3Δ76 (remote)
Space group	C2	C2	C2
<i>a</i> , <i>b</i> , <i>c</i> (Å)	181.38, 38.56, 37.09	91.47, 40.53, 72.47	91.24, 40.21, 72.15
α , β , γ (°)	90.0, 89.3, 90.0	90.0, 102.5, 90.0	90.0, 102.3, 90.0
No. of molecules in unit cell	1	1	1
Solvent content (%)	45.2	44.5	44.5
Resolution range (Å)	45.34–2.15 (2.27–2.15)	42–1.90 (2.00–1.90)	50–1.31 (1.34–1.31)
Total No. of reflections	78062 (11034)	281033 (39088)	413966 (7675)
No. of unique reflections	14192 (2026)	20669 (2973)	61009 (4115)
Completeness (%)	99.8 (99.4)	99.4 (98.4)	98.2 (90.2)
Anomalous completeness (%)	99.2 (98.6)	99.0 (97.0)	
Multiplicity	5.5 (5.4)	13.6 (13.1)	6.8 (1.87)
$\langle I/\sigma(I) \rangle$	12.7 (2.5)	39.1 (15.8)	17.40 (2.1)
R_{merge} (%)	7.3 (79.4)	4.7 (15.5)	5.8 (30.2)
Overall <i>B</i> factor from Wilson plot (Å ²)	30.5	25.9	20.1

EndoIII-3Δ76 with buffer 2 containing 250 mM imidazole. The protein solution was dialyzed overnight at 277 K to remove the imidazole and at the same time TEV protease was added [1:30(*w:w*)] to cleave off the His tag. The protein solution was then applied onto the same Ni-NTA gravity-flow column to remove the cleaved His tag and the His-tagged TEV protease. The cleaved protein showed some intrinsic affinity for the resin and had to be eluted with buffer 2 containing 25 mM imidazole. The flowthrough and low-imidazole wash fractions were then pooled and concentrated using a 10 kDa cutoff filter spin column (Amicon) until a volume of 1–2 ml was reached with a yield of 11–15 mg. The protein was then diluted in buffer 2 with 75 mM NaCl to reduce the salt concentration to 100 mM before ion-exchange chromatography on a Mono S column (GE Healthcare). The enzyme was eluted with a linear salt gradient from 0 to 0.4 M NaCl. The peak fractions were pooled, concentrated and loaded onto a Superdex 75 10/300 size-exclusion column (GE Healthcare) equilibrated with buffer 2. The protein was concentrated to ~12 mg ml⁻¹ and stored at 193 K. The purity, as judged by SDS-PAGE analysis, was estimated to be greater than 95%.

The first crystallization hits for EndoIII-3Δ76 were obtained from commercial screens (Crystal Screen and Crystal Screen 2, Hampton Research) using the hanging-drop vapour-diffusion method in 24-well plates at 293 K. The best crystals were obtained in condition No. 25 of Crystal Screen 2 [0.1 M MES pH 6.5, 1.8 M ammonium sulfate, 0.01 M cobalt(II) chloride hexahydrate]. These crystals were optimized manually and diffraction-quality crystals were obtained in drops consisting of 2 μl precipitation solution [0.1 M MES pH 6.5, 1.4 M ammonium sulfate, 0.01 M cobalt(II) chloride hexahydrate] with 2 μl protein at 6 and 12 mg ml⁻¹ (Table 2). The crystals grew within 2 d to rectangular cuboids with dimensions of ~0.2 × 0.1 × 0.1 mm. Crystals were mounted in cryoloops and soaked in crystallization solution with 30% sucrose as a cryoprotectant before flash-cooling them in liquid nitrogen.

2.5. EndoIII-1 X-ray diffraction analysis and structure determination

EndoIII-1 data were collected on the tunable beamline ID23-1 at the European Synchrotron Radiation Facility (ESRF), Grenoble using an ADSC detector at 100 K (Table 3). A fluorescence scan was performed to localize the peak energy of the absorption edge of the native iron-sulfur cluster to optimize the recording of anomalous signal. The structure of EndoIII-1 was solved with one data set collected at the peak energy of the iron (7.1476 keV, wavelength 1.735 Å) to a maximum resolution of 1.6 Å. The data set was integrated with *XDS* (Kabsch, 2010) and scaled with *SCALA* (Evans, 2006). The EndoIII-1 crystals belonged to the monoclinic space group C2, with unit-cell parameters *a* = 181.38, *b* = 38.56, *c* = 37.09 Å, α = 90.00, β = 89.34, γ = 90.00°, one molecule per asymmetric unit and a solvent content of 45.2% (Table 4). The crystals suffered severe radiation damage, so only the first 400 of a total of 800 frames were used for data processing and structure determination and the resolution was cut back to 2.15 Å. The structure was solved by molecular replacement with *MOLREP* and *Phaser* using the *E. coli* endonuclease III (PDB entry 2abk; Thayer *et al.*, 1995) as a search model (McCoy *et al.*, 2007; Vagin & Teplyakov, 2010; Winn *et al.*, 2011). *Phaser* successfully built a complete chain including residues 13–247. Further model building was performed using *Coot* and the structure is being refined in *REFMAC5* using TLS parameters (Murshudov *et al.*, 2011; Winn *et al.*, 2011).

2.6. EndoIII-3Δ76 X-ray diffraction analysis and structure determination

EndoIII-3Δ76 data were also collected on ID23-1 at the ESRF using an ADSC detector at 100 K (Table 3). The absorption edge of the intrinsic iron-sulfur cluster was determined by a fluorescence scan to optimize the recording of anomalous signal. The structure of EndoIII-3Δ76 was solved with one data set collected at the peak

energy of the iron (7.1476 keV, wavelength 1.735 Å) and refined against a high-resolution native data set (merged data from a high-resolution and a low-resolution pass) collected at a remote energy (11.5 keV, wavelength 1.078 Å) from a second crystal (Table 3). The EndoIII-3Δ76 crystals belonged to the monoclinic space group C2, with unit-cell parameters $a = 91.47$, $b = 40.53$, $c = 72.47$ Å, $\alpha = 90.00$, $\beta = 102.53$, $\gamma = 90.00^\circ$, one molecule per asymmetric unit and a solvent content of 44.5% (Table 4). Data sets were integrated with *XDS* and then scaled with *XSCALE* (Kabsch, 2010). Phasing and initial model building were performed using the automated SAS protocol of *Auto-Rickshaw* (the EMBL Hamburg automated crystal structure-determination platform; Panjikar *et al.*, 2005). The input diffraction data were prepared and converted for use in *Auto-Rickshaw* using programs from the *CCP4* suite (Winn *et al.*, 2011). Based on an initial analysis of the data, the maximum resolution for substructure determination and initial phase calculation was set to 1.90 Å. All four of the heavy-atom positions requested were found using *SHELXD* (Sheldrick, 2010). The correct hand for the substructure was determined using *ABS* (Hao, 2004) and *SHELXE* (Sheldrick, 2010). Initial phases were calculated after density modification using *SHELXE* (Sheldrick, 2010). 88% of the model was built using *ARP/wARP* (Langer *et al.*, 2008). The resulting model consisted of a polypeptide made up of glycine, alanine and serine residues. Further model building was performed using *ARP/wARP* (Langer *et al.*, 2008) with the correct sequence file, and refinement of the structure against the high-resolution data set (1.31 Å) is under way.

3. Results and discussion

In this study, we have successfully established expression, purification and crystallization conditions for two of the three forms of EndoIII from *D. radiodurans*. In the case of EndoIII-1 the intact gene was expressed and purified to homogeneity, while for EndoIII-3Δ76 an N-terminally deleted construct in which the nonconserved N-terminal tail was removed was prepared, since the full-length protein was

poorly soluble and was very unstable during the various chromatographic steps.

This new construct of EndoIII-3 was well expressed and the final yields for both EndoIII-3Δ76 and EndoIII-1 were very satisfactory at >30 mg per litre of culture.

Both recombinant proteins contained a [4Fe–4S] cluster as judged by the brownish colour of the concentrated protein solutions and by their characteristic absorption spectra displaying a peak at 410 nm (Fig. 1).

Initial crystals were obtained for both of the proteins using commercial screens. In the case of EndoIII-1, single crystals obtained directly from the Index screen were used for diffraction experiments, while for EndoIII-3Δ76 manual optimization was needed (Fig. 1). Both precipitant and protein concentrations were varied so as to slow the growth of the crystals and to obtain diffraction-quality crystals. In the end, high-resolution data sets were collected from crystals of both EndoIII-3Δ76 (1.31 Å resolution) and EndoIII-1 (2.15 Å resolution). The EndoIII-3Δ76 crystals belonged to space group C2, with unit-cell parameters $a = 91.47$, $b = 40.53$, $c = 72.47$ Å, $\alpha = 90.00$, $\beta = 102.53$, $\gamma = 90.00^\circ$, and the EndoIII-1 crystals belonged to space group C2, with unit-cell parameters $a = 181.38$, $b = 38.56$, $c = 37.09$ Å, $\alpha = 90.00$, $\beta = 89.34$, $\gamma = 90.00^\circ$.

For phasing purposes, after carrying out a fluorescence scan on the tunable beamline ID23-1 at the ESRF, anomalous signal from the iron was detected for crystals of both EndoIII enzymes, and two complete SAD data sets were collected at the peak energy. In the case of EndoIII-3Δ76, we collected an additional high-resolution data set by combining data from a high-resolution and a low-resolution pass collected at a remote energy (Table 3) to use for refinement of the structure. Interestingly, although these peak data sets were collected in similar ways from relatively large crystals (Fig. 1), the EndoIII-1 crystals suffered from serious radiation damage and the resolution of the final data set was cut to 2.15 Å. The structure of EndoIII-1 was solved by molecular replacement using the *E. coli* endonuclease III as a search model. In contrast, no clear molecular-replacement solutions were obtained for EndoIII-3Δ76, so experimental SAD phasing was performed using the automated *Auto-Rickshaw* platform. Final model building and refinement are ongoing for both these structures.

We expect these structures to provide us with clues as to why the extremely radiation-resistant bacterium *D. radiodurans* possesses three different forms of this essential BER enzyme.

The data for this work was collected on the ID23-1 beamline at the ESRF. We thank the beamline staff for assistance and advice during data collection. This work used the high-throughput crystallization platform of the Grenoble Instruct centre (ISBG; UMS 3518CNRS-CEA-UJF-EMBL) with support from FRISBI (ANR-10-INSE-05-02) and GRAL (ANR-10-LABX-49-01) within the Grenoble Partnership for Structural Biology (PSB). This work was supported by funding from the Research Council of Norway (Synkrotron Program, Project No. 185269) and from the in-house research program of the ESRF. Part of this work was also funded by the CEA in the context of the 'Radiations ionisantes' programme and a Marie Curie Intra-European Fellowship (IEF) for career development through FP7 of the European Commission.

References

- Battista, J. R. (1997). *Annu. Rev. Microbiol.* **51**, 203–224.
 Dimasi, N., Flot, D., Dupeux, F. & Márquez, J. A. (2007). *Acta Cryst.* **F63**, 204–208.
 Evans, P. (2006). *Acta Cryst.* **D62**, 72–82.

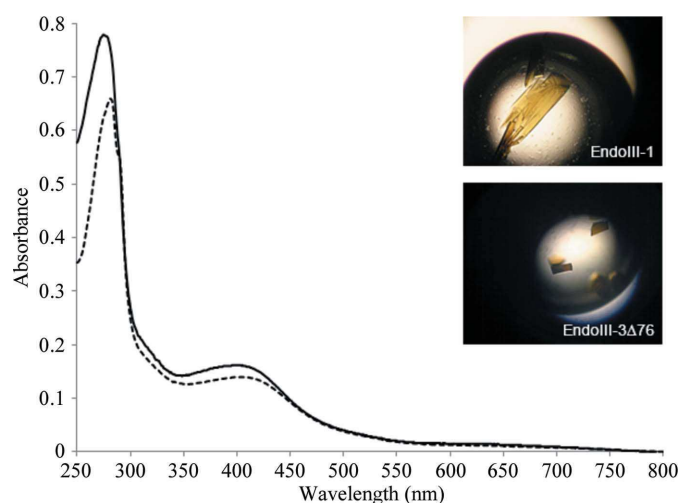


Figure 1
 UV-Vis spectra and typical crystals (insets) of EndoIII-1 and EndoIII-3Δ76. UV-Vis spectra of ~100 μM purified protein in 50 mM Tris–HCl pH 7.5 for EndoIII-1 or 50 mM Tris–HCl pH 8.0 for EndoIII-3Δ76 and 50 mM NaCl were acquired using a Shimadzu UV-1603 spectrophotometer. The spectra show a peak at ~410 nm, which confirms the presence of an iron–sulfur cluster in both EndoIII-1 (continuous line) and EndoIII-3Δ76 (dotted line), which also causes the brown/yellow colour of the protein crystals.

- Hao, Q. (2004). *J. Appl. Cryst.* **37**, 498–499.
- Kabsch, W. (2010). *Acta Cryst.* **D66**, 125–132.
- Krokan, H. E. & Bjørås, M. (2013). *Cold Spring Harb. Perspect. Biol.* **5**, a012583.
- Langer, G., Cohen, S. X., Lamzin, V. S. & Perrakis, A. (2008). *Nature Protoc.* **3**, 1171–1179.
- Makarova, K. S., Aravind, L., Wolf, Y. I., Tatusov, R. L., Minton, K. W., Koonin, E. V. & Daly, M. J. (2001). *Microbiol. Mol. Biol. Rev.* **65**, 44–79.
- McCoy, A. J., Grosse-Kunstleve, R. W., Adams, P. D., Winn, M. D., Storoni, L. C. & Read, R. J. (2007). *J. Appl. Cryst.* **40**, 658–674.
- Moe, E., Hall, D. R., Leiros, I., Monsen, V. T., Timmins, J. & McSweeney, S. (2012). *Acta Cryst.* **D68**, 703–712.
- Murshudov, G. N., Skubák, P., Lebedev, A. A., Pannu, N. S., Steiner, R. A., Nicholls, R. A., Winn, M. D., Long, F. & Vagin, A. A. (2011). *Acta Cryst.* **D67**, 355–367.
- Panjikar, S., Parthasarathy, V., Lamzin, V. S., Weiss, M. S. & Tucker, P. A. (2005). *Acta Cryst.* **D61**, 449–457.
- Sheldrick, G. M. (2010). *Acta Cryst.* **D66**, 479–485.
- Sutherland, B. M., Bennett, P. V., Sidorkina, O. & Laval, J. (2000). *Biochemistry*, **39**, 8026–8031.
- Thayer, M. M., Ahern, H., Xing, D., Cunningham, R. P. & Tainer, J. A. (1995). *EMBO J.* **14**, 4108–4120.
- Vagin, A. & Teplyakov, A. (2010). *Acta Cryst.* **D66**, 22–25.
- Ward, J. F. (1988). *Prog. Nucleic Acid Res. Mol. Biol.* **35**, 95–125.
- Winn, M. D. *et al.* (2011). *Acta Cryst.* **D67**, 235–242.